A Review and Comparison of Lithium-Ion Battery SOC Estimation Methods for Electric Vehicles

Andreas Manthopoulos
AVL Powertrain UK Ltd
andreasmanthopoulos@gmail.com

Xiang Wang
AVL Powertrain UK Ltd
Xiang.Wang@avl.com

***Abstract*—In this research, a Thevenin battery model is proposed considering the hysteresis effect. A general comparison of model-based methods is followed by simulations with different State-of-Charge (SOC) estimation methods i.e., Coulomb Counting, Open Circuit Voltage, Extended Kalman Filter and Adaptive Extended Kalman Filter, Luenberger Observer and Neural Networks based on the same dataset. The results show that the proposed battery model can accurately provide SOC estimation and Adaptive Extended Kalman Filter can provide SOC estimation even with false initialization. Neural Networks deliver a slightly more accurate prediction. However, the requirement of large memory storage can be restricted for some applications.**

Keywords—State of Charge; Battery modelling; hysteresis effect; Coulomb Counting; Open Circuit Voltage; Luenberger Observer; Adaptive Extended Kalman Filter; Neural Network

I. INTRODUCTION

The massive popularity and widely accepted hybrid and electric vehicles led for further development of battery technology. Lithium Ion (Li-ion) is the current leading technology and requires advanced battery management systems (BMSs). The estimation of State of Charge (SOC) is one of the most crucial tasks of a BMS because it indicates the remaining energy inside the battery to power the vehicle. The SOC can be defined as the percentage of the remaining capacity in its maximum available capacity.

Different application of a BMS requires accurate SOC estimation for real-time applications due to safety and efficiency implications. Different methods have been proposed in the literature for the SOC estimation of a battery as a complex electrochemical element. These methods can be categorized under four main groups which are the conventional methods, adaptive filter algorithms, observers and learning algorithms.

For the analysis below, at least a method from each category has been analyzed and evaluated based on a common dataset. Simulations are performed to evaluate and compare the performance of these methods. An equivalent circuit battery model is proposed, and the gathered results are discussed in the final section.

This work is supported by AVL Powertrain UK Ltd.

II. CONVENTIONAL METHODS

In this chapter, conventional methods of battery SOC estimation are investigated, discussing the advantages and challenges of each method as well as the practical implementation. The conventional methods of battery SOC consist of the coulomb counting or ampere-hour counting method, the open circuit voltage method, the impedance and internal resistance method and the electrochemical method.

A. Coulomb Counting

A direct method used to define the SOC (z(t)) is the coulombic counting method. The integration of battery current is described by the following equation:

$$z(t) = z(t_o) - \frac{1}{Q} * \int_{t_0}^{t} (n * I(\tau) - S_d) d\tau \qquad (1)$$

where S_d is the self-discharge rate, n the coulombic efficiency, Q the nominal capacity and $I(t)$ the current (discharge current considered as positive). In addition, $z(t_o)$ denotes the initial SOC at time t_0 , where t_0 is the initial time while t the current time.

Extracting the derivative of SOC from Eq (1) could help the designer to implement the coulomb counting SOC estimation into a state space system.

$$\dot{z}(t) = -\frac{n * I(t) - S_d}{Q} \qquad (2)$$

However, for implementation purposes the conversion of continuous time model into a discrete time ordinary difference equations (ODEs) is necessary. Therefore, Eq (2) can be written in the discrete time as follows:

$$z[k+1] = z[k] - \frac{nT}{Q} i[k] \qquad (3)$$

where the current is considered constant over the sampling interval. The self-discharge rate occurred mainly due to calendric ageing has been found approximately 5% per month for a Lithium-Ion battery [1], while coulombic efficient is estimated as 1.0 during discharging and 0.98 during charging [2]. The coulombic efficiency aims to eliminate the error caused by the initial value of SOC (cumulative effect).

978-1-7281-5414-5/20/$31.00 ©2020 IEEE

Coulombic counting method is widely applied due to its low computational cost, but the cumulative effect and the dependence on the value of the nominal capacity limit the online applications. A periodic capacity calibration is required to reset the maximum capacity. However, it might shorten the battery lifespan [3].

B. *Open Circuit Voltage*

Open Circuit Voltage (OCV) is the battery voltage when the circuit is disconnected from the load [4]. The SOC estimation can be derived only by using the correspondence between SOC and OCV (Fig 1a) either as look-up tables or an analytical expression [5]. However, OCV is also a function of temperature which can be included in the design.

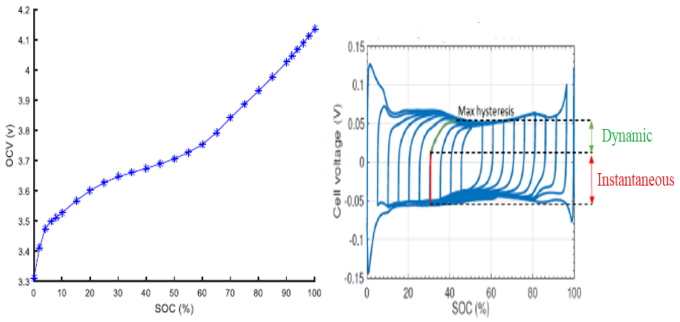

Fig. 1. (a) Open Circuit Voltage vs SOC [5]*; (b) Evidence of hysteresis* [6]

The Open Circuit Voltage method is mainly suitable for offline applications and can be used for SOC initialization for online methods. The main limitation of the method is that the measurement of battery voltage requires sufficient resting time for the battery (hours depending on SOC states, temperature etc.) [7] to reach equilibrium condition [8], otherwise the hysteresis, polarizations and diffusion effects have to be considered [9]. In addition, the relationship between OCV-SOC is not the same for all types of batteries as it depends on battery's material and capacity [10]. Despite the drawbacks some BMS adjust the SOC measurements by using some rest periods due to simplicity.

The hysteresis can be visualized in Fig 1b**,** where the nominal value of OCV has been removed to highlight the effect. It can be noticed that hysteresis can be modelled taking into consideration a dynamic change (marked green) due to SOC changes and an instantaneous change (marked red) when the sign of the current changes. Therefore, a simple model can be introduced by the following equations [6]:

$$h[k+1] = \exp\left(-\left|\frac{ni[k]\gamma T}{Q}\right|\right)h[k] - (1 - \exp\left(-\left|\frac{ni[k]\gamma T}{Q}\right|\right)sgn(i[k]) \quad (4)$$

$$h_i[k] = \begin{cases} sgn(i[k]), & |i[k]| > 0 \\ h_i[k-1], & otherwise \end{cases} \quad (5)$$

$$u_h[k] = M_0 h_i[k] + Mh[k] \quad (6)$$

where h and h_i denotes the state of dynamic and instantaneous hysteresis, respectively, M the maximum absolute value of hysteresis, γ a parameter responsible for tuning the rate of decay, $sgn(i[k])$ forces the stability for both dis/charge, M_0 is the amplitude of instantaneous hysteresis and u_h the output hysteresis voltage. In addition, $h_i[k]$ represents the sign of the current including a memory effect during a rest period [11].

C. *Impedance and Internal Resistance*

The relationship of internal resistance and SOC depends mainly on the temperature and C-rate. The method calculates the resistance of the battery by altering the current for a short period of time and using the battery voltage and current. For online applications the method is called Electrochemical Impedance Spectroscopy (EIS) and except resistances, capacitors and voltage sources employ a Warburg element and a constant phase element (CPE). The impedance element consisting of a resistor and a CPE in parallel is called ZARC or ZC element [12]. SOC can be directly estimated by the relationship of Impedance-SOC with the measured AC signals:

$$R_{EIS}(omega) = \frac{V_{AC}}{I_{Ac}} * e^{if} \quad (7)$$

where V_{AC} , I_{Ac} denotes the measured peak amplitude voltage and current, respectively and f is the phase between them. The calculated magnitude of impedance is indicated by a Nyquist plot and can be compared with the known impedance value.

The change of internal resistance is difficult to be accurately observed due to the nonmonotonic relationship and is more sensitive to temperature rather than SOC changes [13] mainly in the region approximately from 25% to 95% [14]. On the other hand, the use of altering current (AC) causes an unstable SOC and impedance relationship with high cost and also varies with battery types, ageing and temperature [13].

D. *Electrochemical Method*

The SOC can be derived from the estimation of Li concentration in the positive or negative electrodes and reaction overpotentials. Employing partial differential equations which are based on chemical dynamics, thermodynamics and mass transfer [1] for the electrochemical model increases the complexity of the algorithm.

However, to integrate the relevant equations a spatial discretization and linearization of the model is needed. The output of the model is again the terminal voltage, therefore the implementation of an observer or Kalman filter is necessary for the final SOC estimation. Due to the complexity of an electrochemical model there have been several attempts to reduce the order of electrochemical equations for online applications, but produces weak observability of the battery system [15]. Finally, the electrochemical method needs to obtain the impedance spectra of the battery which is difficult to implement in online applications as it is time consuming [16].

III. BATTERY MODELLING

A. Model-Based Method

The development of a battery model is crucial to estimate an accurate online SOC. In order to simulate the battery voltage through the electrical characteristics with any current excitation, Equivalent Circuit Models (ECMs) deploy resistances and RCs.

The ECMs can be used either for SOC estimation through battery parameter identification or with the same way as EIS, called modern control design technique. On the modern control design technique, a predetermined SOC is used to release OCV value and calculate the terminal voltage of the battery (Battery Voltage Model). The last step for the SOC estimation is the deployment of an algorithm (Algorithm Correction) which is responsible for the adjustment of the predetermined SOC value.

B. Equivalent Circuit Model

Therefore, a standalone ECM is not capable to estimate the SOC value, but in co-operation with other methods can produce a highly accurate SOC estimation. An ECM can be represented as a Rint model, a Thevenin model, a GNL, a n-RC model or Fractional Order Model (FOM):

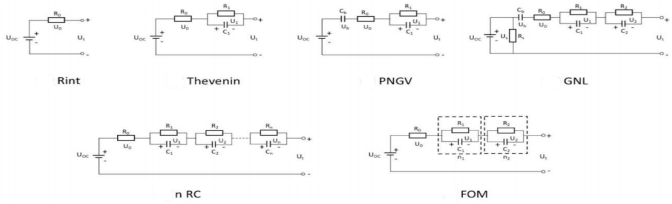

Fig. 2. Electrical equivalent battery models [1]

The behavior of a battery can be explained while the battery is discharged with a current pulse. They can be identified three different parts in the voltage drop, an instantaneous, a delayed or exponential response and a last one at the end of discharge where the OCV is lower due to reduced SOC. The internal resistance of an ECM represents the behavior of the separator inside the battery which is one of the most temperature dependence and causes the instantaneous drop. The series of RC elements in parallel give the overall dynamic response of a battery. The voltage level is represented by a nonlinear or SOC depended voltage source.

The main drawback of a model-based method is that is highly dependent on the model accuracy. In addition, the method requires knowledge about resistances, capacitors and OCV and their relationship with SOC, ageing and temperature variations.

The developed ECM was based in the Thevenin 2-RC method which can be formed with the following equations:

$$V_t = V_{oc} - I * R_i - \sum_{i=1}^{n} V_n \tag{8}$$

$$\frac{dV_n}{dt} = \frac{I}{C_{p,n}} - \frac{V_n}{R_{p,n} * C_{p,n}} \tag{9}$$

where n denotes the number of the RC network, R_i is the internal resistance and $R_{p,n}$, $C_{p,n}$ the polarization resistance and capacity, respectively. The representation of this system in the discrete time can be derived as follows:

$$V_t[k] = V_{oc}(z[k]) - i[k] * R_i - \sum_{i=1}^{n} V_n[k] + u_h[k] \tag{10}$$

$$V_n[k+1] = \exp\left(-\frac{T}{R_{p,n} * C_{p,n}}\right) V_n[k] - R_{p,n}\left(1 - \exp\left(-\frac{T}{R_{p,n} * C_{p,n}}\right)\right) i[k] \tag{11}$$

Therefore, from the discrete-time Eq. (3), (4), (5), (6), (10), (11), considering the hysteresis the following state-space system of the equivalent circuit model can be derived:

$$\begin{bmatrix} V_1[k+1] \\ V_2[k+1] \\ \vdots \end{bmatrix} = \underbrace{\begin{bmatrix} \exp(-\frac{T}{R_{p,1} * C_{p,1}}) & 0 & \dots \\ 0 & \exp(-\frac{T}{R_{p,2} * C_{p,2}}) & 0 \\ \vdots & 0 & \ddots \end{bmatrix}}_{A_{RC}} \begin{bmatrix} V_1[k] \\ V_2[k] \\ \vdots \end{bmatrix} + \underbrace{\begin{bmatrix} R_{p,1}\left(1 - \exp\left(-\frac{T}{R_{p,1} * C_{p,1}}\right)\right) \\ R_{p,2}\left(1 - \exp\left(-\frac{T}{R_{p,2} * C_{p,2}}\right)\right) \\ \vdots \end{bmatrix}}_{B_{RC}} i[k] \tag{12}$$

$$V[k+1] = A_{RC} V[k] + B_{RC} i[k] \tag{13}$$

Therefore, the state equation of the system, which describes all the dynamic effects is formed as follows:

$$\underbrace{\begin{bmatrix} z[k+1] \\ V[k+1] \\ h[k+1] \end{bmatrix}}_{x[k+1]} = \underbrace{\begin{bmatrix} 1 & 0 & 0 \\ 0 & A_{RC} & 0 \\ 0 & 0 & A_h[k] \end{bmatrix}}_{A[k]} \underbrace{\begin{bmatrix} z[k] \\ V[k] \\ h[k] \end{bmatrix}}_{x[k]} + \underbrace{\begin{bmatrix} \frac{-nT}{Q} & 0 \\ B_{RC} & 0 \\ 0 & A_h[k]-1 \end{bmatrix}}_{B[k]} \underbrace{\begin{bmatrix} i[k] \\ sgn(i[k]) \end{bmatrix}}_{u[k]} \tag{14}$$

where,

$$A_h[k] = \exp\left(-\left|\frac{ni[k]\gamma T}{Q}\right|\right) \tag{15}$$

And finally, the output equation:

$$V_t[k] = V_{oc}(z[k]) - i[k] * R_i - \sum_{i=1}^{n} V_n[k] + M_0 h_i[k] + Mh[k] \tag{16}$$

IV. Adaptive Filter Algorithms

Adaptive filter algorithm or non-linear observer are algorithms used for estimation. Through the available measured signals and specifically for BMS mainly by using the measured terminal voltage, the estimated state compared with the measured state and the error is adjusted with an appropriate gain (Fig 3). For the calculation of that gain different methods can be employed. The accuracy and the robustness of the estimation method, and the noise influence can be modified by choosing the most suitable algorithm.

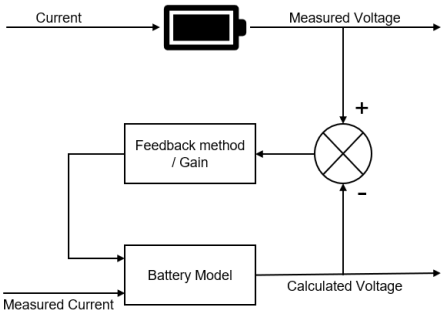

Fig. 3. Block diagram of adaptive algorithm or observer

A. Kalman Filter

Kalman filter is an adaptive filter algorithm to estimate the dynamic states of the battery. More specifically, BMS algorithms use the self-correcting nature of the algorithm to tolerate the variation of current. KF is a linear quadratic estimator which considers the optimal solution to the Bayesian filter under conditions of linear-Gaussian uncertainty and consists of an extremely fast method. However, it is limited to linear and uni-modal systems. While the system operates, KF estimates and corrects the new state. The mathematical equations of the method are presented below:

$$x_{k+1} = A_k x_k + B_k u_k + w_k \quad (17)$$

$$y_k = C_k x_k + D_k u_k + v_k \quad (18)$$

where A, B, C, D denote the covariance matrices which describe the dynamics of the system, x is the system states (mean), u is the control vector (which describes how we expect the system to transition between states), y, the measurement output prediction, w, the process noise or disturbance, v, the measurement noise and k, the time index.

The whole procedure takes place in two step process with a state prediction and a state update step. The state prediction step predicts the states at future time x_{k+1}, considering the known estimate and a correction for known influences. Additionally, that step includes the prediction of the covariance, where the predicted covariance ($P_{k|k-1}$) is made from the old uncertainty plus some additional one (Q_k) from the environment. Using the predicted states and covariance, the innovation matrix and covariance can be extracted taking into consideration the process noise Q. Therefore, the Kalman gain is calculated, which essentially indicates the relation between our expected covariance and measured covariance. The Kalman gain indicates whether our actual value is close to predicted or measured value. Q and R can be found as a normal probability distribution of process and measurement noise respectively. The second step updates the state vector and covariance according to the innovations and Kalman Gain (how well our measurement matches our prediction). High measurement noise means low Kalman Gain and vice versa.

Summary of the Kalman filter algorithm

- State-space model:

$$x_{k+1} = A_k x_k + B_k u_k + w_k$$
$$y_k = C_k x_k + D_k u_k + v_k$$

- Initialization: For $k = 0$, set

$$\hat{x}_0 = E[x_0]$$
$$P_0 = E[(x_0 - \hat{x}_0)^T (x_0 - \hat{x}_0)]$$

- Computation: For $k = 1, 2, \ldots$, compute
  - State estimate propagation
    $$\hat{x}_{k|k-1} = A_{k-1} x_{k-1} + B_{k-1} u_{k-1}$$
  - Error covariance propagation
    $$P_{k|k-1} = A_k P_{k-1} A_k^T + Q_k$$
  - Kalman gain matrix
    $$K_k = P_{k|k-1} C_k^T (C_k P_{k|k-1} C_k^T + R_k)^{-1}$$
  - State estimate update
    $$\hat{x}_k = \hat{x}_{k|k-1} + K_k (y_k - C_k \hat{x}_{k|k-1} - D_k u_k)$$
  - Error covariance update
    $$P_k = (I - K_k C_k) P_{k|k-1}$$

B. Extended Kalman Filter

To estimate SOC by applying an adaptive algorithm the battery model is necessary. Due to the nonlinearity of the battery model KF cannot be implemented directly and a linearization process must take place. An adaptive algorithm capable to linearize the model at each time step is called Extended Kalman Filter. EKF linearizes the battery model with partial derivatives and the first order Taylor series expansion.

EKF is very similar to KF using the same methodology of prediction and correction step. The innovation covariance and Kalman Gain governing equations are almost identical with KF, differing only in A and C matrices. The nonlinear system can be modelled as:

$$x_{k+1} \approx \hat{A}_k x_k + f(\hat{x}_k, u_k) - \hat{A}_k \hat{x}_k + w_k \quad (19)$$

$$y_k \approx \hat{C}_k x_k + g(\hat{x}_k, u_k) - \hat{C}_k \hat{x}_k + v_k \quad (20)$$

where $\hat{A}_k$ is the Jacobian Matrix, the first order derivative of Taylor series. Therefore, the only changes of EKF innovation covariance and Kalman Gain equations are the replacement of A_k and C_k with the linearized $\hat{A}_k$ and $\hat{C}_k$, respectively. Also, in the covariance update C_k is substituted by $\hat{C}_k$ and in the state estimation update $\hat{y}_k = g(\hat{x}_{k|k-1}, u_k)$.

Notwithstanding the above advantages, this is a computationally intensive method and requires a good initial estimate. However, the most crucial one is the lack of accuracy in highly nonlinear systems such as battery system.

C. Adaptive Extended Kalman Filter

EKF relies on the accuracy of the battery model and the predetermined variables of the system noise (mean value and covariance matrix) [17]. Inaccurate setting of those variables may result in noticeable errors and divergence in SOC estimation [18]. Therefore, Adaptive EKF (AEKF) is used for online SOC estimation to enhance the accuracy of the EKF by adaptively updating the process and measurement noise covariance. The whole procedure is similar to EKF, however in the end of every computation cycle the algorithm updates the process and measurement noise matrixes.

D. Fading Kalman Filter

Another adaptive algorithm is the Fading Kalman Filter (FKF), which main function is the limitation of the necessary memory by using a fading factor. Therefore, the algorithm provides the feasibility and simplicity required for real-time applications combined with insensitivity to noise covariance variations and capability of compensating any modelling error [1].

FKF is similar to original Kalman filter, however it differentiates in the error covariance propagation. It uses a constant scaling a which controls the fading memory effect. More specifically, alpha controls how much the designer wants the filter to forget past measurements. Choosing $a = 1$ yields in an identical performance to the Kalman filter and a typical value for a fading memory application might be 1.01 [19].

E. Unscented Kalman Filter

As mentioned, EKF provides a good accuracy for the first and second order of non-linear model, but its performance is pure for high non-linear state-space models due to the limitation of a first order accuracy of propagated mean and covariance. Considering the aforementioned reasons, the Unscented Kalman Filter (UKF) was developed [13]. The UKF follows a similar approach to the EKF. However, in order to avoid the setback of Taylor series expansion, it employs a discrete time filtering algorithm and unscented transform able to solve any filtering problem [20]. The UKF is the most well-known filter from Kalman filters also known as Sigma-Point Kalman Filter (SPKF).

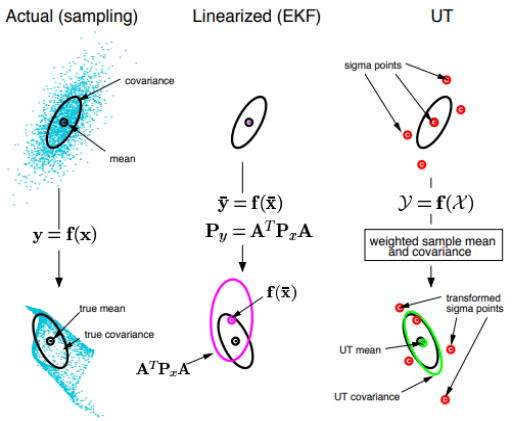

Fig. 4. Example of UT for mean and covariance propagation [21]

EKF, as mentioned, uses only one point which is the mean and linearizes every time step around that point. Whereas, UKF uses a set of points (called sigma points) including the mean and approximates around them. The precision of the approximation is better with a higher number of points, but on the other hand the necessary computational power is increasing. An overview of the basic adaptive algorithms such as EKF and UKF can be shown in Fig 4, where the basic principles and UKF capability to work in higher nonlinear systems are highlighted.

V. Observers

Occasionally, the state variables (velocities, positions, temperatures, voltages, etc.), which characterize a dynamic system, cannot be directly measured. An observer is capable to estimate those useful variables by using only the knowledge of variables that can be measured.

A. Luenberger Observer

An observer operates according to Fig 3, where it uses the previously calculated state equation to estimate the battery terminal voltage. After a comparison with the real cell, the extracted error between estimated and real measurement is used for correction with the help of a gain vector L. The estimated model with the correction is described by the following equations:

$$\dot{\hat{x}} = A\hat{x} + Bu + L(y - \hat{y}) \quad (21)$$

$$\hat{y} = C\hat{x} + Du \quad (22)$$

The observer aims to eliminate the error over time and achieve similar behavior between the developed model for estimation and the real cell. Therefore, the main objective is to minimize the following error [22]:

$$e = x - \hat{x} \quad (23)$$

$$\dot{e} = \dot{x} - \dot{\hat{x}} = (A - LC)e \quad (24)$$

To ensure convergence of the error toward zero, the matrix formed by $(A - LC)$ must have its eigenvalues inside the unit disk. With A and C matrices already known from the system, vector L has to be chosen in order to respect that condition. In addition, the conditions of observability must be fulfilled between A and C matrices in order to ensure the arbitrary pole placement of the closed loop. Then, the correction vector L is adjusted to achieve poles of the $(A - LC)$ matrix which corresponds to system's pole and converges asymptotically to zero. However, Luenberger observer suffers from low accuracy and requires trial and error tuning of the feedback gain [23].

B. Proportional-Integral Observer

Proportional-Integral Observer (PIO) has been applied as a replacement of feedback control system and gain [24]. According to the definition of PIO, it is designed as follows:

$$\dot{\hat{x}} = A\hat{x} + Bu + K_p(y - \hat{y}) + K_{i2}w \quad (25)$$

$$\dot{w} = K_{i1}(y - \hat{y}) \quad (26)$$

where w is defined as the integral of the difference between actual and estimated output (terminal voltage) $(y - \hat{y})$, while

vectors K_p and K_{i1}, K_{i2} are the proportional and integral gains, respectively and replace the gain vector L of Luenberger observer. The PI method has an easy implementation due to its simple structure combined with high efficiency and precision, however require trial and error tuning of the gains.

C. Sliding Mode Observer

Sliding Mode Observer (SMO) employs enhanced tracking control to ensure stability and robustness of the system against model uncertainties and environmental disturbances [25]. The model is using the state equation as output state, which is broken down to the observer equations in the next stage [25]. The observer of the system is defined:

$$\dot{\hat{x}} = A\hat{x} + Bu + L\, sgn(e_y) \qquad (27)$$

where $e_y = y - C\hat{x} = Ce_x$ with $e_x = x - \hat{x}$ and L represent vectors of switching gains. The dynamics of the observer error e_x are described as follows:

$$\dot{e}_x = Ax + w(t) - A\hat{x} - L\, sgn(e_y) \qquad (28)$$

The sliding-mode observer shows robustness by maintaining the sliding regime despite the dynamical disturbances and retaining tracking properties caused by the sliding regime [26].

VI. Learning Algorithms

A. Artificial Neural Network

Data-driven control methods are becoming a niche area for SOC estimation as an alternative to ECMs and electrochemical models avoiding uncertain external operating conditions of batteries and most importantly the internal complex chemical reaction process. The artificial neural network (ANN or NN) is a learning algorithm, which has the self-learning skills and adaptability to illustrate a complex non-linear battery model. The NN takes terminal voltage, current, and temperature (when it is considered) as input and SOC as output to construct the structure of the NN network of battery. The advantage of this method is the capability of working in high non-linear battery conditions. Nevertheless, the algorithm needs to store a large amount of data for training and validation which requires large memory storage and may overload the entire system [25].

Different NN can be found in the literature, even with combinations with other algorithms such as EKF [27]. In [28] the researcher used the same dataset. The training process of the backward pass was performed by an optimization method called Adam, which updates the weights and biases and Rectified Linear Units (ReLU) used for activation functions. The NN created with 3 layers; where the first two layers contained 4 neurons and the last fully-connected layer contained 1 neuron, corresponding to 36 network weights and with averaging parameter set to 400.

VII. Results & Simulations

For the gathered results and simulation purposes a dataset of a 2.9Ah Panasonic 18650PF battery at 25ºC and a cut-off voltage of 2.5V was used. Therefore, the temperature dependence was not explored at this point of testing. A drive cycle called Urban Dynamometer Driving Schedule (UDDS) also known as US FTP-72 and LA-4 cycle was performed in the power profile of a Ford F150 35KWH. The SOH (State of Health) of the battery before the test was calculated 96.5%.

The first tested method was the CC method and without the reset of the nominal capacity the absolute maximum error (AME) of SOC was 3.67%. As it can be noticed from the Fig 5b the fading capacity is the main reason of that cumulative error. With the reset of the capacity the AME was significantly decreased to 0.159% which indicates the importance of the capacity calibration and the best achievable performance of an algorithm. In addition, the RMSE (Root Mean Square Error) was calculated 2.1055 and 0.0947 for the CC method without and with the reset of the capacity respectively.

The equation of RMSE is presented below:

$$RMSE = \sqrt{\frac{1}{n}\sum_{i=1}^{n}(y_i - \hat{y}_i)^2} \qquad (29)$$

where y_i denotes the real measurement, $\hat{y}_i$ the estimated value and n the time index.

During the simulations the self-discharge rate was neglected, the initial SOC assumed known for CC method and the coulombic efficiency was defined one for both discharging and charging. The method is highly depended on the initial SOC, therefore requires additional control designs for initialization and elimination of cumulative error.

The results of the OCV method can be visualized in Fig 5c where the AME was 5.13%, whereas the RMSE 4.51%. The effect of the non-modelled hysteresis OCV in combination with the non-measured disturbances and noise could explain the pure performance of this method. Additionally, the OCV cannot be measured online due to the necessity of resting period without load and the employment of an ECM or EIS was necessary.

The proposed ECM was implemented and used for the developed model-based approaches. A factor with high influence in the accuracy of the algorithm was the RC parameter values. The 2 RC network was used considering RC values measured in the AVL lab. The RC values and the internal resistance are highly affected by the temperature and SOC. However, at this point of testing the temperature variations were not considered. The second factor with high influence in the accuracy was the relationship between terminal voltage and SOC. Since this relationship was nonlinear, a linear approximation every 0.1 SOC was used with the last 10% of the battery divided into three regions as the nonlinearity was higher there. From OCV vs SOC graph of charge and discharge the dynamic and instantaneous hysteresis M and M_0, respectively and the maximum absolute value of hysteresis, γ were extracted for simulation reasons. Fig 5a denotes a good estimation of terminal voltage over the SOC range. A small deviation of the estimated value from the real one was noticed

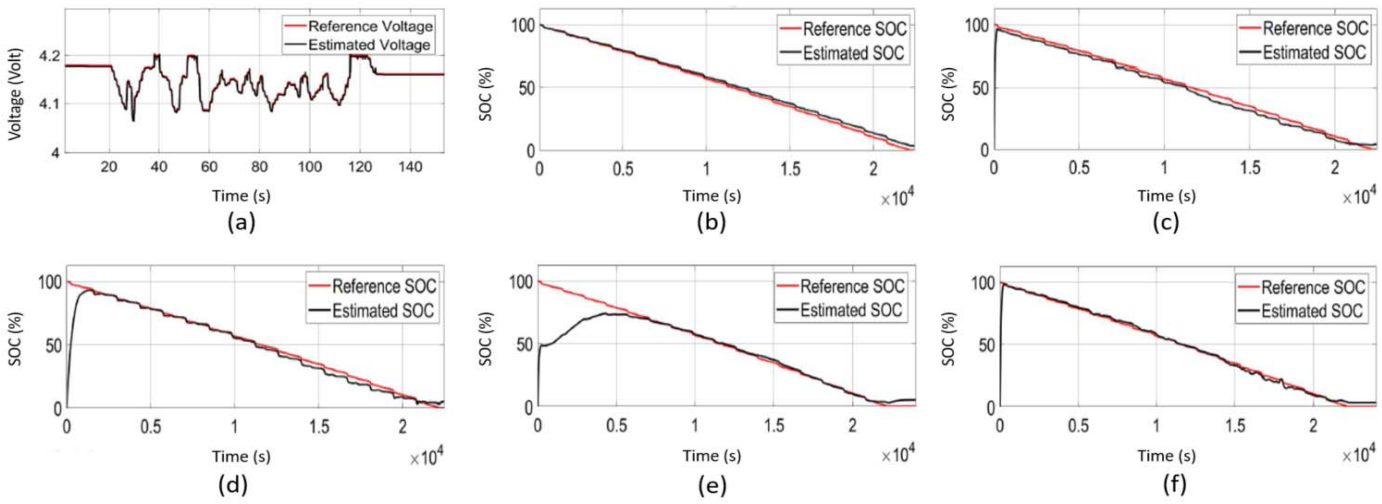

Fig. 5. The simulation results of the developed SOC estimation methods: (a) Terminal Voltage of model-based approach with proposed ECM; (b) CC SOC estimation; (c) OCV SOC estimation; (d) Luenberger Observer SOC estimation; (e) EKF SOC estimation; (f) AEKF SOC estimation

at the end of battery's discharge as it represents the region with the highest nonlinearity.

A Luenberger Observer was implemented with the pole placement technique ($[-0.01 \ -0.2 \ -0.1]$) resulting to a gain vector L. The simulations indicate an AME of 5.59% and an RMSE of 8.73. However, the converge speed was low (18 minutes) with an initial SOC of 0%. The choice of this initial value was due to safety reasons in case the vehicle has already very low SOC.

The EKF as well as the AEKF were tested taking into consideration the state space system which was formulated previously. We noticed that the algorithms estimate the terminal voltage despite the high nonlinearity with an approximate accuracy of 50mV. Both algorithms were initiated with 0% SOC as it is assumed that there is no previous knowledge. The EKF provides an accuracy of 3.21% AME, however the converge speed is 103 minutes resulting to 14.33% RMSE. On the other hand, the AEKF provides a convergence speed of 1 minute. However, the high nonlinearity of the battery led to 3.88% AME. Generally, the error was less than 2% in the most SOC regions except the region between 10% and 20% where it can be noticed that OCV curve exhibits a more nonlinear relationship with SOC and the influence of hysteresis effect is greater.

All the gathered results compared with a NN developed in [28]. In that research the simulations conducted with a 2 different driving cycles the HWFET and US06. The presented and compared results are from US06 drive cycle as it is the expansion of the used one (UDDS); however, the battery testing took place for the same battery cell, in the same lab leading to a comprehensive comparison.

The results indicate that the NN has a similar performance with EKF in terms of AME, however the NN did not require any amount of time for convergence. Comparing its performance with the best developed method of AEKF in terms of accuracy, converge speed and false initialization, it can be noticed only a difference in accuracy of 0.53% (AME). The difference is relatively small while the requirement of a large memory storage for a NN should be taken into consideration. Nevertheless, further investigation on learning algorithms should be conducted in the future. Table I sums all the gathered results of the developed methods compared to the NN.

TABLE I. ERROR OF SOC ESTIMATION

Method	*Max Error (%)*	*RMSE (%)*
CC with reseted Capacity	0.16	0.09
CC	3.67	2.11
OCV	5.13	4.51
EKF	3.21	14.33
AEKF	3.88	4.14
Luenberger	5.59	8.73
NN	3.14	0.61

VIII. CONCLUSIONS

Different model-based estimation methods including Coulomb Counting, Open Circuit Voltage, Extended Kalman Filter and Adaptive Extended Kalman Filter, Luenberger Observer have been applied and compared with a Neural Network to estimate the SOC of Lithium-Ion batteries for electric vehicles. The electrical behavior of the battery is simulated by a proposed second order RC model with hysteresis effect. In addition, the basic theories of all the model-based methods are presented by highlighting advantages and disadvantages. The Adaptive Extended Kalman Filter was better in terms of converge speed, adaptiveness in a false initialization with an absolute maximum error of 3.88%. The Neural Network study with the same dataset provides an absolute maximum error of 3.14% and further research should be conducted in terms of computational power, storage, different learning algorithms methods and temperature variations.

Acknowledgment

Battery testing was performed at the University of Wisconsin-Madison by Dr. Phillip Kollmeyer and in the facilities of AVL List GmbH.

References

[1] R. Zhang *et al.*, "State of the art of lithium-ion battery SOC estimation for electrical vehicles," *Energies*, vol. 11, no. 7, 2018.

[2] K. W. E. Cheng, B. P. Divakar, H. Wu, K. Ding, and H. F. Ho, "Battery-management system (BMS) and SOC development for electrical vehicles," *IEEE Trans. Veh. Technol.*, 2011.

[3] F. Leng, C. M. Tan, R. Yazami, and M. D. Le, "A practical framework of electrical based online state-of-charge estimation of lithium ion batteries," *J. Power Sources*, 2014.

[4] G. Fathoni, S. A. Widayat, P. A. Topan, A. Jalil, A. I. Cahyadi, and O. Wahyunggoro, "Comparison of State-of-Charge (SOC) estimation performance based on three popular methods: Coulomb counting, open circuit voltage, and Kalman filter," in *Proceedings of the 2nd International Conference on Automation, Cognitive Science, Optics, Micro Electro-Mechanical System, and Information Technology, ICACOMIT 2017*, 2018.

[5] I. Baccouche, S. Jemmali, A. Mlayah, B. Manai, and N. E. Ben Amara, "Implementation of an improved Coulomb-counting algorithm based on a piecewise SOC-OCV relationship for SOC estimation of Li-ion battery," *Int. J. Renew. Energy Res.*, 2018.

[6] "Equivalent Circuit Cell Model Simulation | Coursera." [Online]. Available: https://www.coursera.org/learn/equivalent-circuit-cell-model-simulation. [Accessed: 07-Nov-2019].

[7] I. Snihir, W. Rey, E. Verbitskiy, A. Belfadhel-Ayeb, and P. H. L. Notten, "Battery open-circuit voltage estimation by a method of statistical analysis," *J. Power Sources*, 2006.

[8] L. Zheng, L. Zhang, J. Zhu, G. Wang, and J. Jiang, "Co-estimation of state-of-charge, capacity and resistance for lithium-ion batteries based on a high-fidelity electrochemical model," *Appl. Energy*, 2016.

[9] M. A. Roscher and D. U. Sauer, "Dynamic electric behavior and open-circuit-voltage modeling of LiFePO 4 -based lithium ion secondary batteries," *J. Power Sources*, 2011.

[10] T. Dong, J. Li, F. Zhao, Y. Yi, and Q. Jin, "Analysis on the influence of measurement error on state of charge estimation of LiFePO4 power Battery," in *ICMREE2011 - Proceedings 2011 International Conference on Materials for Renewable Energy and Environment*, 2011.

[11] G. L. Plett, "Extended Kalman filtering for battery management systems of LiPB-based HEV battery packs - Part 1. Background," *J. Power Sources*, 2004.

[12] J. R. MacDonald, "Comparison of the universal dynamic response power-law fitting model for conducting systems with superior alternative models," *Solid State Ionics*, 2000.

[13] Y. Zheng, M. Ouyang, X. Han, L. Lu, and J. Li, "Investigating the error sources of the online state of charge estimation methods for lithium-ion batteries in electric vehicles," *Journal of Power Sources*. 2018.

[14] L. Lu, X. Han, J. Li, J. Hua, and M. Ouyang, "A review on the key issues for lithium-ion battery management in electric vehicles," *Journal of Power Sources*. 2013.

[15] A. Bartlett, J. Marcicki, S. Onori, G. Rizzoni, X. G. Yang, and T. Miller, "Electrochemical Model-Based State of Charge and Capacity Estimation for a Composite Electrode Lithium-Ion Battery," *IEEE Trans. Control Syst. Technol.*, 2016.

[16] Z. Zou, J. Xu, C. Mi, B. Cao, and Z. Chen, "Evaluation of model based state of charge estimation methods for lithium-ion batteries," *Energies*, 2014.

[17] R. Xiong, H. He, F. Sun, and K. Zhao, "Evaluation on State of Charge estimation of batteries with adaptive extended kalman filter by experiment approach," *IEEE Trans. Veh. Technol.*, 2013.

[18] H. He, X. Zhang, R. Xiong, Y. Xu, and H. Guo, "Online model-based estimation of state-of-charge and open-circuit voltage of lithium-ion batteries in electric vehicles," *Energy*, 2012.

[19] K. C. Lim, H. A. Bastawrous, V. H. Duong, K. W. See, P. Zhang, and S. X. Dou, "Fading Kalman filter-based real-time state of charge estimation in LiFePO 4 battery-powered electric vehicles," *Appl. Energy*, 2016.

[20] F. Yang, Y. Xing, D. Wang, and K. L. Tsui, "A comparative study of three model-based algorithms for estimating state-of-charge of lithium-ion batteries under a new combined dynamic loading profile," *Appl. Energy*, 2016.

[21] E. A. Wan and R. Van Der Merwe, "The unscented Kalman filter for nonlinear estimation," in *IEEE 2000 Adaptive Systems for Signal Processing, Communications, and Control Symposium, AS-SPCC 2000*, 2000.

[22] T. He, D. Li, Z. Wu, Y. Xue, and Y. Yang, "A modified luenberger observer for SOC estimation of lithium-ion battery," in *Chinese Control Conference, CCC*, 2017.

[23] X. Tang, B. Liu, F. Gao, and Z. Lv, "State-of-Charge Estimation for Li-Ion Power Batteries Based on a Tuning Free Observer," *Energies*, 2016.

[24] X. Tang, Y. Wang, and Z. Chen, "A method for state-of-charge estimation of LiFePO<inf>4</inf> batteries based on a dual-circuit state observer," *J. Power Sources*, 2015.

[25] M. A. Hannan, M. S. H. Lipu, A. Hussain, and A. Mohamed, "A review of lithium-ion battery state of charge estimation and management system in electric vehicle applications: Challenges and recommendations," *Renewable and Sustainable Energy Reviews*. 2017.

[26] X. Chen, W. Shen, Z. Cao, A. Kapoor, and I. Hijazin, "Adaptive gain sliding mode observer for state of charge estimation based on combined battery equivalent circuit model in electric vehicles," *Proc. 2013 IEEE 8th Conf. Ind. Electron. Appl. ICIEA 2013*, no. April, pp. 601–606, 2013.

[27] Z. Chen, S. Qiu, M. A. Masrur, and Y. L. Murphey, "Battery state of charge estimation based on a combined model of extended kalman filter and neural networks," in *Proceedings of the International Joint Conference on Neural Networks*, 2011.

[28] E. Chemali, P. J. Kollmeyer, M. Preindl, and A. Emadi, "State-of-charge estimation of Li-ion batteries using deep neural networks: A machine learning approach," *J. Power Sources*, 2018.